Binding Studies Using Ion-Selective Electrodes. Examination of the Picrate–Albumin Interaction as a Model System

Theodore K. Christopoulos[1]

Laboratory of Analytical Chemistry, University of Athens, 104 Solonos Street, Athens 106 80, Greece

Eleftherios P. Diamandis*[,2]

Department of Clinical Biochemistry, Toronto Western Hospital, 399 Bathurst Street, Toronto, Ontario M5T 2S8, Canada

We are studying the binding of ligands to macromolecules by using ligand ion selective electrodes as transducers. The picrate–bovine albumin interaction is examined in detail as a model system. A picrate ion selective electrode is used to monitor the free picrate concentration directly in the presence of albumin and bound ligand. The binding parameters are estimated and the effect of protein concentration, ionic strength, pH, and temperature is studied. The experimental data are interpreted with a specially designed computer program that performs nonlinear least-squares fitting of the generalized Scatchard model with an infinite number of classes of binding sites directly to the raw potentiometric data. The binding parameters (binding constant and maximum number of ligands that can be bound), the nonspecific binding as well as their standard deviations are estimated by this program. The principles described can be used for the potentiometric study of any ligand–binder interaction.

INTRODUCTION

The interaction of small molecules (ligands) with biological macromolecules has attracted increasing interest during the last 20–30 years because it was realized that such interactions are involved in many regulatory and defence mechanisms, in metabolic pathways and in the expression of the pharmacologic action of many drugs. More specifically, it is now well-known that most drugs, during their transport through the blood circulation, bind reversibly to blood constituents, e.g. albumin, globulins, lipoproteins, etc. This binding influences both the intensity and duration of the pharmacologic action because only the free drug is able to reach the sites of the pharmacologic action (receptors) or drug metabolism (*1*).

All binding studies are focused on the determination of the binding parameters i.e. (a) the maximum number of ligands that can be bound to a macromolecule and (b) the value of the binding constant. Other interesting aspects of binding are the structure of the binding sites and the forces that are involved in this process. The analytical methodology that has been applied to study binding phenomena is used primarily to measure the concentration of either the free (nonbound) or the bound ligand, usually under equilibrium conditions, in solutions–mixtures of known total concentration of both the ligand and the macromolecule (binder). These methods are either indirect or direct. In the indirect methods, the amount of bound or free ligand is measured after a physical separation of the two fractions. In the direct methods, this is not necessary because binding results in a change of a physical property of the ligand, e.g. in the absorption or emission spectrum.

Examples of indirect methods include equilibrium (*2–4*) or dynamic (*5*) dialysis, ultrafiltration (*6*), gel filtration (*6*), and high-performance liquid chromatography (*7*). Examples of direct methods include absorption, fluorescence, nuclear magnetic resonance, or circular dichroism spectroscopy (*2–4*).

Ion-selective electrodes (ISE) are electrochemical transducers able to monitor directly the free ion activity (concentration) in a solution that contains both the free and the bound form. During the last 15 years, many studies have focused on the factors that affect the ISE response in complex biological solutions containing proteins and cells like serum and whole blood. These studies address the practical problems of measuring ions like H^+, Na^+, K^+, Cl^-, Ca^{2+}, Mg^{2+}, and Li^+ in biological fluids without or with minimal sample pretreatment or dilution. Currently, many such ions are measured routinely in biological fluids using ISE, which is now the preferred methodology over flame photometry (*8*, *9*).

Although the results of monitoring free ion concentration in protein solutions using ISE are very encouraging, the use of such transducers in binding studies involving proteins as binders and inorganic or organic ions as ligands is very limited. The Mg^{2+} and Ca^{2+} ISE have been used to study the binding of these ions to bovine and human serum albumin (*10*, *11*). Similar studies have been published for Cu^{2+} (*12*, *13*). In these studies, the determination of the binding parameters was carried out either by graphical methods or by least-squares fitting of the hyperbola of the Scatchard plot to the experimental data. Similar methods were used to determine the parameters for the binding of bile acids to bovine serum albumin using an ISE for bile acids (*14*). An ISE for flufenamic acid has also been reported and its response studied in the presence of bovine albumin, but no binding parameters were determined (*15*). The ISE for dodecyl sulfate and octyl or decyl sulfate were used to study the binding of these ions to bovine albumin (*16*) and β-lactoglobulin (*17*), respectively. The estimation of the bound anion was based on the increase of the critical micelle concentration in the presence of the binder.

In this paper, we are examining the binding of ligands to macromolecules by using ligand ISE. In order to demonstrate the capabilities of the proposed system, we are using the picrate–bovine serum albumin interaction as a model. A picrate ISE (*18*) is used to monitor the free concentration of the ligand in the presence of albumin. The binding parameters are estimated, and the effect of the protein concentration, ionic strength, pH, and temperature on the estimation of the binding parameters is studied.

We have also designed a computer program which performs nonlinear least-squares fitting of the generalized Scatchard model (ref 19, infinite number of classes of binding sites) directly to the raw (untransformed) experimental data, i.e.,

[1] Present address: Department of Clinical Biochemistry, Toronto Western Hospital, 399 Bathurst St., Toronto, ON M5T 2S8, Canada.
[2] Also: Department of Clinical Biochemistry, University of Toronto, 100 College St., Toronto, ON M5G 1L5, Canada.

0003-2700/90/0362-0360$02.50/0

to the pairs of electrode potential and total ligand concentration. The binding parameters and the nonspecific binding as well as their standard deviations are estimated by this program.

EXPERIMENTAL SECTION

Apparatus. The picrate anion selective electrode was used with a single junction Ag–AgCl electrode as the external reference (Orion Model 90-01-00). Potential readings were obtained with a Corning Research pH/mV meter (Model 12) and recorded simultaneously on a strip-chart recorder (Radiometer) equipped with a high sensitivity unit (REA-112). The pH measurements were carried out with a combination glass electrode (Radiometer). A double-walled 50-mL beaker was used as the reaction cell. During binding studies, the temperature was kept constant (±0.1 °C) and the reaction mixtures were stirred with the aid of a magnetic stirrer.

Reagents. All chemicals used were of analytical reagent grade and deionized distilled water was used for solution preparation.

Buffers. The buffers used were phosphate, 0.1 M, for pH 6.5, 7.0, 7.4, 8.0, and 11.5 and borate, 0.1 M, for pH 9.0. The buffers were prepared by dissolving sodium dihydrogen phosphate or boric acid and adjusting the pH with a 10 M sodium hydroxide solution.

Sodium Picrate Stock Solution (0.100 M). Air-dried picric acid (22.91 g) (Fluka) was mixed with ~800 mL of water and the pH was adjusted with 10 M NaOH to 6.0. The final volume was then adjusted to 1 L with water. The solution was stored in an amber bottle at room temperature. More dilute solutions were prepared as needed, by dilution with buffer solutions.

Bovine Serum Albumin (BSA) Solutions. Bovine serum albumin (Cohn fraction V, albumin content 96–99 %, Sigma) was used. The albumin content of solutions is checked by weighing the residue after drying a certain volume for 2 h at 105 °C. Dilute BSA solutions for binding studies are prepared in various buffers as needed. These solutions are stored for no more than a week at 4 °C.

Sodium Picrate–Bovine Serum Albumin Mixed Solutions. These are prepared by mixing appropriate volumes of picrate and BSA solutions, as described in detail later.

Procedures. *Picrate-Ion Selective Liquid Membrane Electrode.* The preparation of the liquid ion exchanger and the characteristics of the picrate ion selective electrode have been described elsewhere (*18*). The liquid ion exchanger consists of the tetrapentylammonium–picrate ion pair, dissolved in 2-nitrotoluene (0.01 M). An Orion liquid membrane electrode body (Model 92) was used as the electrode assembly with the Millipore LCWPO 1300 PTFE porous membrane. The PTFE membrane was cut to the appropriate size and a stack of four was used to avoid any leakage of the organic phase. The internal reference solution was 0.1 M NaCl–0.01 M sodium picrate (saturated with silver chloride). When not in use, the electrode was kept in a 10^{-2} M solution of sodium picrate.

Calibration Curve of the Picrate ISE. A 20.0-mL volume of the appropriate buffer solution is pipetted into the thermostated reaction cell, the picrate ISE and the reference electrode are immersed in it, and stirring at a constant rate is started. After 2–3 min, various increments of a 3.00×10^{-2} M sodium picrate solution are added. The electromotive force (emf) readings are recorded after stabilization to ±0.1 mV (it takes about 30 s and remains constant for at least 2 min). The constant term, E', and the slope, S, of the Nernst equation are calculated by regression analysis of the linear part of the graph.

Potentiometric Study of the Picrate–BSA Interaction. A 20.0-mL volume of a BSA solution (solution A) in the appropriate buffer is pipetted into the thermostated reaction cell, the picrate–ISE and the reference electrode are immersed in it, and stirring at a constant rate is started. After 2–3 min, an aliquot of a mixed solution that contains sodium picrate (0.03 or 0.1 M total concentration depending on the experiment) and BSA at a concentration equal to that of solution A is added. The volume added is such that the emf reading becomes equal (±1 mV) to that of the largest emf value of the linear part of the calibration curve (this value corresponds to a 2×10^{-5} M concentration of free picrate). Afterward, various increments of the mixed solution are added until the emf recorded reaches the lowest value of the linear part of the calibration curve (this corresponds to a 10^{-2} M concentration of free picrate). The emf readings are recorded after stabilization to ±0.1 mV following each addition (we typically wait about 30 s but readings remain unchanged for at least 2 min after stabilization). During such binding experiments, the total BSA concentration is kept constant irrespective of the dilution that occurs due to the addition of picrate solution.

THEORY AND CALCULATIONS

The free picrate concentration, F, after each addition, is calculated from the emf readings and the equation of the calibration curve. The bound picrate concentration, B, after each addition, is calculated from the equation

$$B = T - F \tag{1}$$

where T is the total picrate concentration after each addition.

In this work, we use the generalized Scatchard model (*19*) to describe the binding phenomena. The protein is considered to have an m number of distinct classes of independent and noninteracting binding sites. Class i contains an n_i number of individual sites that have the same affinity for the ligand. The site binding constant, K_i, characterizes the sites of the ith class. The concentration of bound ligand, B, is related to the above parameters as shown by eq 2 (*19*), where P_t is the total protein concentration. The second term of this equation takes account for the nonspecific binding of the ligand to the protein molecule, Ns being the nonspecific binding parameter (*20*, *21*).

$$B = \sum_{i=1}^{m} \frac{n_i K_i F}{1 + K_i F} P_t + \mathrm{Ns}\, F \tag{2}$$

After F is calculated from the calibration curve and B from eq 1, the Scatchard plot is constructed (B/F vs B). From this plot the Ns parameter can be estimated by performing linear least-squares fitting of the B/F vs B data which are located at the last part of the plot. In this area, the plot is approximately parallel to the horizontal axis. The estimation of Ns in this manner is based on the fact that if the free ligand concentration becomes too high, the B/F ratio reaches a constant value that is equal to Ns (eq 2).

The knowledge of Ns allows for the construction of the corrected Scatchard plot, which is the plot of B_{spec}/F vs B_{spec} (B_{spec} specifically bound ligand). The value of B_{spec} is equal to $B - \mathrm{Ns}\,F$. From the corrected Scatchard plot, approximate values for the binding parameters n and K are obtained by using the method of limiting slopes and intercepts described in detail in ref 22 assuming a model with two classes of binding sites. These graphically obtained parameters are used as initial estimates in a nonlinear least-squares fitting process that calculates the statistically "true" values. This process is described in detail below.

Nonlinear Least-Squares Fitting of the Generalized Scatchard Model Directly to the Raw Experimental Data. The total picrate concentration after each addition is selected as the independent variable and the emf as the dependent variable. The binding parameters and the total picrate concentration determine each time the free picrate concentration in the solution and this in turn determines the expected (calculated) emf, E_c. Because of the random errors that unequivocally accompany every analytical measurement, the observed emf, E_i, differs from the theoretically calculated one and the following equation holds:

$$E_i = (E_c)_i + e_i \tag{3}$$

where e_i is the experimental error at the ith emf measurement. The most probable values of the parameters n_j, K_j ($j = 1, ..., m$), and Ns are those that minimize the sum of the squares of residuals.

$$\Phi = \sum_{i=1}^{N} w_i [E_i - (E_c)_i]^2 = \sum_{i=1}^{N} w_i e_i^2 \tag{4}$$

where N is the number of the experimental points and w_i is the statistical weight accompanying the ith emf measurement ($w_i = \sigma_i^{-2}$, σ_i is the standard deviation of the ith emf value). The function Φ is minimized when its partial derivatives with respect to the parametes become zero, i.e.

$$\partial\Phi/\partial\theta_l = 0 \qquad \text{for } l = 1, ..., p \ (p = 2m + 1) \qquad (5)$$

with $\theta_l = n_l$ for $l = 1, ..., m$, $\theta_l = K_l$ for $l = m + 1, ..., 2m$ and $\theta_{2m+1} = Ns$. Calculating the partial derivatives from eq 4 and introducing them in eq 5 give

$$\frac{\partial\Phi}{\partial\theta_l} = -2\sum_{i=1}^{N} \frac{w_i e_i \partial(E_c)_i}{\partial\theta_l} \qquad \text{for } l = 1, ..., p \qquad (6)$$

which can be expressed in matrix notation as

$$\mathbf{J}^T\mathbf{W}\mathbf{e} = \mathbf{0} \qquad (7)$$

where $\mathbf{J}$ is the $N \times p$ Jacobian matrix with elements $J_{ij} = \partial(E_c)_i/\partial\theta_j$ (the symbol T as an exponent states the transpose of a matrix), $\mathbf{W}$ is a $N \times N$ diagonal matrix with $W_{ii} = w_{ii}$, and $\mathbf{e}$ is the $N \times 1$ vector of the residuals e_i. Relationship 6 (or 7) is in fact a nonlinear system of p equations with p unknowns that is solved by an iterative process (*23*, *24*). If $\theta^{(0)}$, $(\mathbf{Ec})_{T,\theta^{(0)}}$ and θ, $(\mathbf{Ec})_{T,\theta}$ are the initial (guess) and the final (solution) parameter vectors, respectively, with the corresponding emf vectors, then a Taylor series expansion about $(\mathbf{Ec})_{T,\theta}$ gives

$$(\mathbf{Ec})_{T,\theta} = (\mathbf{Ec})_{T,\theta^{(0)}} + \mathbf{J}\Delta\theta \qquad (8)$$

where terms higher than the first order have been neglected. $\Delta\theta$ is the parameter correction vector.

Subtituting the vector $\mathbf{e}$ from eq 3 into eq 7 yields

$$\mathbf{J}^T\mathbf{W}[\mathbf{E} - (\mathbf{Ec})_{T,\theta}] = 0 \qquad (9)$$

After substituting $(\mathbf{Ec})_{T,\theta}$ from eq 8 into eq 9 and rearrangement yields:

$$(\mathbf{J}^T\mathbf{W}\mathbf{J})\Delta\theta = \mathbf{J}^T\mathbf{W}\mathbf{e} \qquad (10)$$

Relationship 10 is a linear system of p equations with p unknowns. The correction vector can be provided by solving this system. The new parameter vector is then given by

$$\theta^{(1)} = \theta^{(0)} + \Delta\theta \qquad (11)$$

When the above algorithm (Gauss–Newton) was applied for the fitting of the Scatchard model to the potentiometric binding data, it did not always converge and many times there was an increase rather than a decrease in the sum of squares of residuals during the iterative process. This happened because this algorithm does not assure that the $(\mathbf{J}^T\mathbf{W}\mathbf{J})$ matrix will be in each iteration a positive definite. To overcome this problem, we applied the Marquardt–Levenberg modification (*25*) where the parameter correction vector is calculated by solving the linear system

$$(\mathbf{J}^T\mathbf{W}\mathbf{J} + \lambda\mathbf{D})\Delta\theta = \mathbf{J}^T\mathbf{W}\mathbf{e} \qquad (12)$$

where λ is a positive number and $\mathbf{D}$ a diagonal matrix with elements $D_{ii} = (J^TWJ)_{ii}$.

The iterative process has two loops. In the external one, initial parameter estimates are introduced and the vector of the expected emf values is calculated. The elements of the matrix $\mathbf{J}$ and vector $\mathbf{e}$ are then calculated and also the sum of the squares of residuals. Afterward, the elements of the $(\mathbf{J}^T\mathbf{W}\mathbf{J})$ matrix and of the vector $\mathbf{J}^T\mathbf{W}\mathbf{e}$ (eq 12) are calculated. At this point, the internal loop is started. An initial value is assigned to the parameter λ, the linear system (eq 12) is solved (by the Gauss–Jordan elimination method), and the correction vector $\Delta\theta$ derived is added to the parameter values yielding better values. The new value of Φ is then calculated and is compared with the previous one. If it is greater, then the internal loop is repeated by increasing λ until an acceptable correction vector (which will decrease Φ) is yielded. In this case, the internal loop closes and a new external loop is started by entering the new parameter values as starting ones. The iterative process is terminated (converged) when the corrections of the parameters are less than 0.01% of their current values. An interactive computer program written in BASIC (for the IBM PC and for the AMSTRAD CPC computers) performs the potentiometric binding data treatment, i.e., the calibration of the electrode, the calculation of the initial estimates of the binding parameters, and the nonlinear least-squares fitting. In addition, the calibration graph, the saturation plot, and the Scatchard plot are also constructed by the computer along with the corresponding calculated curves. Furthermore, the user has the option to fit several Scatchard models (variable number of classes of sites) searching for the best one without reloading the binding data.

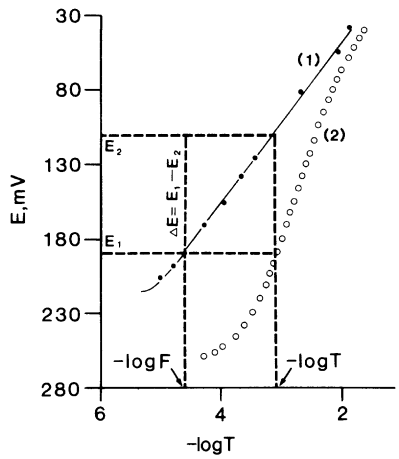

Figure 1. Calibration curves of the picrate ISE (1) and a plot of emf vs −log T in the presence of BSA at a concentration of 32.0 g/L (2).

The calculation of the expected emf value for each experimental point is carried out by first estimating the free picrate concentration as a function of the total picrate concentration and of the current values of binding parameters. This is accomplished by the Newton–Raphson approximative method (*26*) and is described in Appendix A. In Appendix B, the calculation of the partial derivatives of the electrode potential with respect to binding parameters is presented for the general form of the Scatchard model (infinite number of sites).

RESULTS AND DISCUSSION

The principle of the application of ion-selective electrodes for the study of the binding of ionic ligands to macromolecules (e.g. proteins) is based on the fact that in a solution containing protein molecules, free ionic ligand, and protein bound ionic ligand, the ISE responds only to the free ionic ligand species. Because of their highly hydrophilic character, neither the protein molecules nor the protein-bound ions can penetrate into the organic solvent of the electrode membrane to cause a change in the emf.

A typical calibration curve (E vs −log F) of the picrate ISE as well as a plot of the emf vs −log T in the presence of BSA are presented in Figure 1. Once the picrate binds to albumin it cannot be sensed by the electrode; thus, the observed emf is much higher in the presence of albumin (curve 2), in comparison to the same total picrate concentration and absence of albumin from the measuring solution. The theoretical slope of the emf vs log T curve is given at any point by the derivative of the emf with respect to log T. The following equation holds (chain rule):

$$\frac{dE}{d(\log T)} = \frac{dE}{d(\log F)} \frac{d(\log F)}{dF} \frac{\partial F}{\partial T} \frac{dT}{d(\log T)} \qquad (13)$$

Table I. Influence of the Protein Concentration on the Binding of Picrate to BSA[a]

BSA, g/L	n_1	$10^{-3}K_1$, M^{-1}	n_2	$10^{-3}K_2$, M^{-1}	Ns	SD_{re},[b] mV
20.0	1.64 (0.02)	39.0 (1.1)	4.7 (0.2)	0.89 (0.04)	0.27 (0.07)	0.2
32.0	1.83 (0.04)	42.1 (0.8)	4.9 (0.1)	0.92 (0.03)	0.39 (0.01)	0.1
50.0	1.70 (0.03)	37.7 (0.9)	4.4 (0.1)	0.93 (0.04)	0.59 (0.01)	0.2

[a] Numbers in parentheses are the standard deviations of the parameter values. [b] SD_{re} is the standard deviation of residuals as defined in the text.

Table II. Influence of Ionic Strength on the Binding of Picrate to BSA[a]

[NaCl], M	n_1	$10^{-3}K_1$, M^{-1}	n_2	$10^{-3}K_2$, M^{-1}	Ns	SD_{re}, mV
0.01	1.60 (0.04)	36.9 (1.5)	4.2 (0.1)	1.27 (0.09)	0.21 (0.01)	0.3
0.05	1.67 (0.03)	34.5 (0.9)	4.6 (0.1)	1.00 (0.05)	0.28 (0.01)	0.1
0.10	1.78 (0.02)	32.2 (0.5)	5.0 (0.1)	0.91 (0.03)	0.20 (0.01)	0.3
0.20	1.74 (0.04)	28.3 (0.8)	3.6 (0.1)	1.09 (0.09)	0.26 (0.01)	0.3

[a] See footnote of Table I for further explanations and abbreviations.

Table III. Effect of pH on the Binding of Picrate to BSA[a]

pH	n_1	$10^{-3}K_1$, M^{-1}	n_2	$10^{-3}K_2$, M^{-1}	Ns	SD_{re}, mV
6.5	2.03 (0.02)	44.4 (0.9)	5.4 (0.1)	0.78 (0.03)	0.42 (0.01)	0.1
7.0	1.83 (0.02)	42.1 (0.8)	4.9 (0.1)	0.92 (0.03)	0.39 (0.01)	0.1
7.4	1.63 (0.02)	38.7 (0.8)	4.7 (0.1)	0.88 (0.04)	0.27 (0.01)	0.1
8.0	1.58 (0.01)	39.4 (0.5)	5.2 (0.1)	0.78 (0.02)	0.32 (0.01)	0.1
9.0	1.39 (0.03)	40.4 (1.3)	3.3 (1.0)	1.25 (0.08)	0.39 (0.01)	0.2
10.0	1.54 (0.05)	26.3 (1.4)	5.7 (1.0)	0.43 (0.10)	0.13 (0.01)	0.5
11.5	1.60 (0.03)	20.3 (0.7)	10.3 (0.5)	0.22 (0.02)		0.4

[a] See footnote of Table I for further explanations and abbreviations.

Given that $dE/d(\log F) = S$, $d(\log F)/dF = 1/2.3F$, and $dT/d(\log T) = 2.3T$ we have

$$\frac{dE}{d(\log T)} = S\frac{T}{F}\frac{\partial F}{\partial T} \tag{14}$$

Equation 14 is general. When no binder (BSA) is present, $T = F$ and the slope of the E vs log T curve equals the electrode slope. In the presence of a binder, the derivative is calculated by substituting T and $\partial F/\partial T$ from eq A1 and A2 (Appendix A) into eq 14 which finally gives

$$\frac{dE}{d(\log T)} = S\frac{\sum_{i=1}^{m}\frac{n_iK_iF}{1+K_iF}P_t + (Ns+1)F}{\sum_{i=1}^{m}\frac{n_iK_iF}{(1+K_iF)^2}P_t + (Ns+1)F} \tag{15}$$

In eq 15, the denominator is always smaller than the numerator because the term $1 + K_iF > 1$. Therefore, $dE/d(\log T)$ is always greater or equal to S in absolute terms, in the presence or absence of the binder, respectively (see Figure 1, curves 2 and 1). The above equations hold only in the area of linear response of the electrode. A simple graphical way for the calculation of the free ion concentration after each addition is also shown in Figure 1. The B/F ratio (ordinate of Scatchard plot) is then directly derived from the equation

$$B/F = 10^{-\Delta E/S} - 1 \tag{16}$$

where ΔE is shown in Figure 1 and S is the electrode slope. The binding of picrate to BSA was studied at three different protein concentrations, i.e. at 20.0, 32.0, and 50.0 g/L. Typical Scatchard plots are presented in Figure 2. It is obvious that at high picrate concentration, the plots, instead of intersecting the horizontal axis at points indicating the total concentration of binding sites, become parallel to the axis due to the nonspecific binding of picrate to BSA. In Table I, we present the values of binding parameters as estimated by nonlinear least-squares fitting of the Scatchard model with two classes

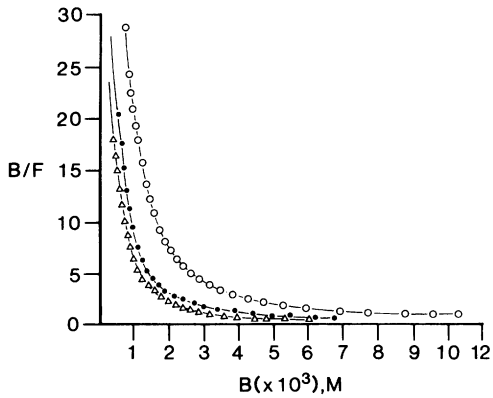

Figure 2. Potentiometric study of the binding of picrate to BSA at different BSA concentrations: Scatchard plots at BSA concentrations of (△) 20.0, (●) 32.0, and (○) 50.0 g/L. The theoretical Scatchard curves (parameter values taken from Table I) are drawn over the experimental points.

of binding sites to the experimental data. It can be observed that the number of binding sites and the binding constants are practically independent of protein concentration. The last column of Table I shows the standard deviation of residuals calculated after the convergence of the iterative process. These numbers are of the same magnitute as the expected error in the measurement of the emf providing strong evidence that the model chosen is correct.

The influence of ionic strength on the binding was studied at a constant BSA concentration of 32.0 g/L by adding NaCl at final concentrations of 0.01, 0.05, 0.10, and 0.20 M. Scatchard plots at various ionic strengths were constructed in a manner similar to that of Figure 2. The values of binding parameters are presented in Table II. Ionic strength does not affect significantly these values. The dependence of picrate/BSA association on the pH was studied at a BSA concentration of 32.0 g/L using the appropriate buffers. Scatchard plots at various pH values were constructed in a

Table IV. Effect of Temperature on the Binding of Picrate to BSA[a]

Temp, °C	n_1	$10^{-3}K_1$, M^{-1}	n_2	$10^{-3}K_2$, M^{-1}	Ns	SD_{re}, mV
10.0	1.78 (0.02)	107.5 (2.2)	4.3 (0.1)	2.99 (0.06)	0.40 (0.01)	0.2
15.2	1.83 (0.02)	83.9 (2.4)	4.2 (0.1)	2.12 (0.06)	0.23 (0.01)	0.2
20.2	1.82 (0.02)	52.6 (1.1)	4.5 (0.1)	1.51 (0.05)	0.24 (0.01)	0.2
30.0	1.72 (0.02)	40.5 (0.7)	4.2 (0.1)	1.26 (0.04)	0.20 (0.01)	0.2
40.3	1.64 (0.01)	29.9 (0.4)	3.7 (0.1)	1.04 (0.03)	0.20 (0.01)	0.1

[a] See footnote of Table I for further explanation and abbreviations.

manner similar to that of Figure 2. The values of the binding parameters are presented in Table III. A significant decrease of both binding constants is observed by increasing the pH above 9.0. In the pH range studied (pH 6.5–11.0), picric acid is completely dissociated (pK_a = 0.38). The decrease in the affinity of protein for picrate by increasing pH above 9.0 is expected since at such high pH values the ϵ-amino groups of lysine are gradually becoming deprotonated. This effect does not favor the attraction of the picrate anion to the BSA molecule. It is generally accepted in the literature that by increasing pH, the ability of albumin to bind anionic ligands decreases (*27*).

The effect of temperature on the binding was studied at 10.0, 15.2, 20.2, 30.0, and 40.3 °C (BSA concentration 32.0 g/L and pH = 7.4). Scatchard plots for each temperature were constructed. Analytical results are presented in Table IV. With decreasing temperature, both binding constants increase. This observation suggests that picrate binding to both classes of sites is an exothermic reaction. The number of binding sites remains practically constant.

From the results presented in Tables I–IV, it can be concluded that the nonspecific binding increases with increasing protein concentration and decreases with increasing temperature and pH reaching zero value at highly alkaline solutions (pH 11.0). Nonspecific binding can be considered as an accumulation of picrate ions on the protein surface because of weak interactions. The incorporation of a term that accounts for nonspecific binding in the general Scatchard model (eq 2) is mandatory for the fitting of the model to the data, especially at high picrate concentrations. This term has also been used previously (*20*, *21*) when binding was studied by radioisotopic techniques. In Figure 3, the percent of bound picrate, $100B/T$ the percent of nonspecifically bound picrate, 100 NsF/T, and the percent of specifically bound picrate, $100(B - \text{Ns}F)/T$, are presented as a functon of the negative logarithm of the free picrate concentration. In fact, this plot shows the extent of nonspecific binding in the concentration range covered. Nonspecifically bound picrate is kept under 10% of total picrate in the range of free picrate concentration from 2×10^{-5} to 3×10^{-3} M (i.e. over a 100-fold range), then increasing rapidly to 17% of total picrate when the free concentration becomes 10^{-2} M (i.e. for only a 3-fold increase in free concentration). In Figure 3, the distribution of bound picrate between the two classes of binding sites of BSA during an experiment is also shown. This is expressed as the percentage of the total picrate concentration that is bound to the first or the second class as a function of −log F.

In Figure 4, saturation plots of BSA (i.e. plots of r = specifically bound picrate/P_t as a function of −log F) at 10.0 and 40.3 °C are shown. The theoretical saturation curves were also constructed by using the binding parameters from Table IV. Saturation plots have been considered (*28*, *29*) as the most objective means for testing the completeness of the binding study and the adequacy of the concentration range covered. It has been theoretically proven (*30*, *31*) that it is necessary to cover a range of 75% of the entire saturation curve to get adequate information for the assignment of the appropriate model to the binding data. As is shown in our experiments

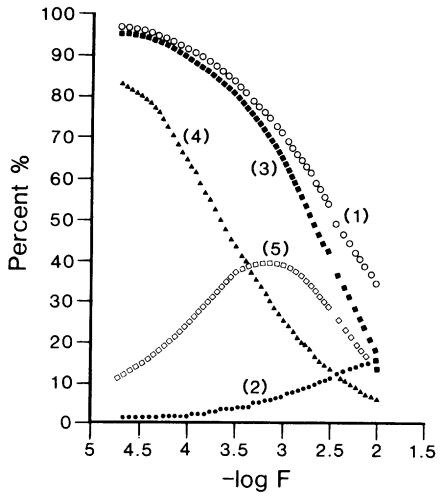

Figure 3. Graphical presentation of various fractions of bound picrate vs −log F during the binding study: (1) percent of totally bound picrate; (2) percent of nonspecifically bound picrate; (3) percent of specifically bound picrate; (4) percent of picrate bound to the first class; (5) percent of picrate bound to the second class of binding sites.

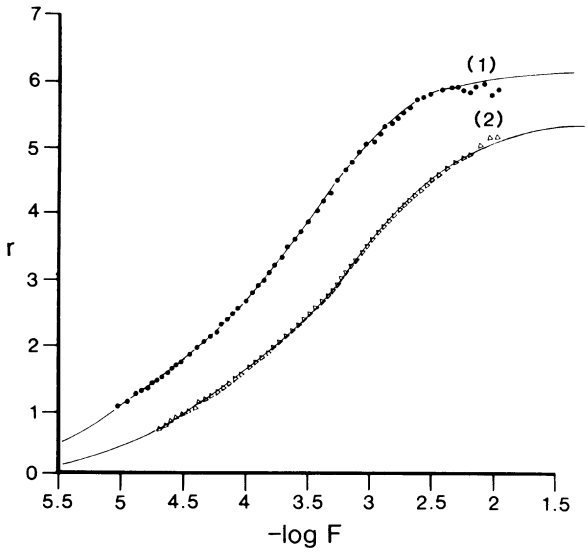

Figure 4. Plots of BSA saturation with picrate at 10° (1) and 40.3 °C (2), respectively. The theoretical saturation curves are drawn over the experimental points.

(Figure 4), a range of about 3 decades of free picrate concentration was covered. This corresponds to a wide saturation range of BSA from 16.6% to 94.9% at 10 °C and from 12.7% to 95.3% at 40.3 °C.

In the present work, the binding experiments were carried out as titrations of the protein with the anionic ligand. With this technique, we have avoided possible errors that may occur due to small changes in E' after frequent removing, washing, and reimmersing the ISE from one solution to the other. This happens when experimental protocols using various mixtures of protein–ligand are used to derive data. The presence of

BSA in the reaction mixture did not change the time needed for the stabilization of the electrode potential (to ±0.1 mV) after each addition of picrate (<30 s). Therefore, it can be concluded that the picrate–BSA association is a rapid reaction completed in less than 30 s. In order to prove that the presence of protein does not cause any deleterious effect to either the picrate ISE membrane or the liquid junction of the reference electrode, we performed calibration curves before and immediately after binding experiments carried out at a 50 g/L BSA concentration. The values for the constant term of the Nernst equation were −72.1 and −72.6 mV and those for the electrode slope were −59.1 and −59.4 mV/decade before and after such binding experiments, respectively. These findings also suggest that there is no significant drift of the electrode response during a compete binding experiment (lasting approximately 60 min).

The contribution of BSA to the ionic strength of the measured solution can be estimated by assuming that the negative charges on the protein molecule (~17 at pH 7.4) (*27*) behave like monovalent anions (*11*). Therefore, a bovine serum albumin concentration of 7.46×10^{-4} M (50 g/L), which is the maximum concentration used in our experiments, causes an additional ionic strength of $I = 6.3 \times 10^{-3}$ M in the measured solution. This contribution is not significant because all experiments were performed in 0.1 M buffer solutions. From these findings, it is concluded that the activity coefficient of the anionic ligand is practically the same in the presence or absence of BSA. It is thus possible to calculate the free picrate concentration in BSA solutions by directly using the equation of the calibration curve.

One contribution of the present work is that it provides a complete and statistically correct treatment of potentiometric data for studies involving the interaction of ionic ligands with macromolecules. Earlier treatments of potentiometric binding data have been based either on graphical procedures (*10–12*) or on least-squares treatment (*13*, *14*) by using B/Pt as the dependent variable and F as the independent variable. There are many graphical approaches that are commonly used for the analysis of such data e.g. the Scatchard plot (*19*), the Benesi–Hildebrand plot (*32*), the Klotz plot (*33*), and the Hill plot (*34*). These methods facilitate transformation of the data into a straight line representation. However, a straight line only results under the simplest binding reaction mechanism and these methods do not generalize to more complicated binding models (e.g. for two or more classes of sites). In addition, the graphical analysis of results always contains some degree of subjectivity. Calculation of binding parameters by least-squares treatment is generally the recommended method. However, the choice of the dependent and independent variables is important for the purpose of satisfying statistical guidelines. A regression analysis has to be performed with the assumption that the independent variable is error-free. In the case of potentiometric data, assuming that the uncertainty in the emf measurement is σ_E (constant) and applying the error propagation law (*35*), we can calculate the uncertainties of the coordinates (B/F and B) of the Scatchard plot as follows

$$\sigma_B = \sigma_F = \frac{2.3\sigma_E}{S}F \tag{17}$$

and

$$\sigma_{(B/F)} = \frac{2.3\sigma_E}{S}\frac{T}{F} \tag{18}$$

where S is the electrode slope.

In Figure 5, a simulated Scatchard plot is shown along with the experimental uncertainties which are caused by an error of $\sigma_E = 2$ mV in the measured electrode potential. The bars

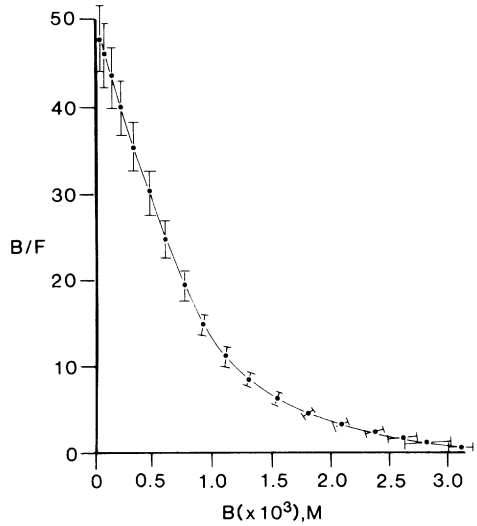

Figure 5. A simulated Scatchard plot along with the experimental uncertainties caused by an error of $\sigma_E = 2$ mV in the emf measurement: $n_1 = 2$; $K_1 = 50\,000\ \mathrm{M}^{-1}$; $n_2 = 5$; $K_2 = 1500\ \mathrm{M}^{-1}$; $P_t = 4.78 \times 10^{-4}$ M.

shown correspond to 1 standard deviation on both the ordinate and the abscissa of the plot. From eqs 17 and 18 and from Figure 5, it is clear that the measurement errors appear in both the independent and the dependent variable and, also, are highly correlated and nonuniform.

For these reasons, the application of common least-squares programs (linear or nonlinear) directly to the Scatchard plot coordinate system is always statistically incorrect and often yields results which are inferior even to those obtained by graphical techniques. The plots of B vs F or F/B vs F as well as the double reciprocal plot ($1/B$ vs $1/F$) are for the same reasons inappropriate for direct regression analysis even if a simple straight line represents the experimental data.

In this work, the original (untransformed) raw potentiometric data, i.e., the electrode potential vs total ion concentration were analyzed by nonlinear least-squares treatment. In this system, the independent variable is practically error-free and the measurement error is restricted to the dependent variable (emf). We used graphical techniques (Scatchard plots) only for presentation of the data and for making initial estimates of the binding parameters. A list of the computer program with sample data and outputs can be obtained by writing to the authors.

The picrate binding to serum albumin was first studied by Teresi and Luck (*36*) using equilibrium dialysis. A very narrow total picrate concentration range (from 5.0×10^{-7} to 2.5×10^{-6} M) was covered. Therefore, a model of only one class of binding sites was assumed. Parameter values of $n = 6$ and $K = 1.26 \times 10^5\ \mathrm{M}^{-1}$ were found by a graphical technique.

Analytical application of the picrate/albumin association was first reported by the authors (*37*, *38*). In these reports, the picrate ISE was used for the quantitative determination of albumin in plasma, serum, and whole blood but the estimation of binding parameters was not performed.

The application of ion selective electrodes for the study of the binding of ions to biological macromolecules offers a number of significant and unique advantages over the existing methodologies. First, the measurement of the free ion in the presence of the bound ion is carried out continuously without the need for separation procedures and without any disturbance of the chemical equilibrium of the system. Furthermore, binding studies can be accomplished in a wide concentration range since ISE response usually covers about 3 decades of the free ion concentration (range of 10^{-5} to 10^{-2} M is typical for most liquid-membrane ISE). In addition, by

the proposed "titration" technique, a large number of experimental points can be obtained in a short time (30–60 s per experimental point). Finally, this method is especially useful in cases where binding does not entail changes of the spectral characteristics of either the macromolecule and/or the ligand. A disadvantage of the proposed potentiometric method is that it does not provide direct information about the nature of the binding sites and of the interactions that are responsible for the phenomenon. It is mostly useful for the estimation of binding parameters.

The picrate–albumin association was used in the present study only as a model. The method described can be extended for any ion–macromolecule interaction. Especially, in view of the many drug ion selective electrodes that have been reported in the literature (*39*), we suggest the use of the above potentiometric methodology for the study of the binding of drugs to serum proteins.

APPENDIX

A. Calculation of the Free Ion Concentration. During the iterative nonlinear fitting process, it is necessary to calculate the free ion concentration corresponding to each experimental point, whenever new parameter values are derived. From the current binding parameter values and the total ion concentration at each experimental point, the free ion concentration is calculated by solving the equation

$$T = \sum_{i=1}^{m} \frac{n_i K_i F}{1 + K_i F} P_t + (\mathrm{Ns} + 1)F \qquad \text{(A1)}$$

using the Newton–Raphson method of successive approximations (*26*).

We start the calculations from the last experimental point (highest total ion concentration) and use this value as initial guess. For the other points, the calculated free concentration of the previous point is taken as initial guess. The general expression of the derivative of T with respect to F at the ith point is

$$\frac{\partial T_i}{\partial F_i} = 1 + \sum_{j=1}^{m} \frac{n_j K_j P_{ti}}{(1 + K_j F_i)^2} + \mathrm{Ns} \qquad \text{(A2)}$$

B. General Expressions for the Partial Derivatives of the Electrode Potential with Respect to the Binding Parameters. The expressions shown below have derived for any number of binding sites and include the case of nonspecific binding. The following equation holds (chain rule)

$$\frac{\partial E_i}{\partial \theta_j} = \frac{\mathrm{d}E_i}{\mathrm{d}(\log F_i)} \frac{\mathrm{d}(\log F_i)}{\mathrm{d}F_i} \frac{\partial F_i}{\partial \theta_j} \qquad \text{(B1)}$$

$$j = 1, \ldots, 2m + 1$$

$$i = 1, \ldots, N$$

where θ_j are the binding parameters. Derivatization of the Nernst equation and substitution to eq B1 give

$$\frac{\partial E_i}{\partial \theta_j} = \frac{S}{2.3F_i} \frac{\partial F_i}{\partial \theta_j} \qquad \text{(B2)}$$

The partial derivatives of F with respect to the binding parameters are calculated indirectly as follows:

$$\frac{\partial F_i}{\partial \theta_j} = -\frac{\partial T_i/\partial \theta_j}{\partial T_i/\partial F_i} \qquad \text{(B3)}$$

Combination of eqs B2 and B3 gives

$$\frac{\partial E_i}{\partial \theta_j} = -\frac{S}{2.3F_i} \frac{\partial T_i/\partial \theta_j}{\partial T_i/\partial F_i} \qquad \text{(B4)}$$

The partial derivatives of T with respect to the parameters are calculated by derivatizing eq A1 with respect to n and K, respectively

$$\frac{\partial T_i}{\partial n_j} = \frac{K_j F_i P_{ti}}{1 + K_j F_i} \qquad \text{(B5)}$$

$$\frac{\partial T_i}{\partial K_j} = \frac{n_j F_i P_{ti}}{(1 + K_j F_i)^2} \qquad \text{(B6)}$$

The partial derivative of T with respect to Ns is

$$\partial T_i/\partial \mathrm{Ns} = F_i \qquad \text{(B7)}$$

By substituting the $\partial T_i/\partial F_i$, $\partial T_i/\partial n_j$, $\partial T_i/\partial K_j$, and $\partial T_i/\partial \mathrm{Ns}$ from eqs A1, B5, B6, and B7, respectively, to eq B4, the following analytical expressions for the partial derivatives are obtained:

$$\frac{\partial E_i}{\partial n_j} = -\frac{SK_j P_{ti}}{2.3\,(1 + K_j F_i)\left[1 + \sum_{l=1}^{m} \frac{n_l K_l P_{ti}}{(1 + K_l F_i)^2} + \mathrm{Ns}\right]} \qquad \text{(B8)}$$

$$\frac{\partial E_i}{\partial K_j} = -\frac{Sn_j P_{ti}}{2.3(1 + K_j F_i)^2\left[1 + \sum_{l=1}^{m} \frac{n_l K_l P_{ti}}{(1 + K_l F_i)^2} + \mathrm{Ns}\right]} \qquad \text{(B9)}$$

$$\frac{\partial E_i}{\partial \mathrm{Ns}} = -\frac{S}{2.3\left[1 + \sum_{l=1}^{m} \frac{n_l K_l P_{ti}}{(1 + K_l F_i)^2} + \mathrm{Ns}\right]} \qquad \text{(B10)}$$

Registry No. Picric acid, 88-89-1.

LITERATURE CITED

(1) Reidenberg, M. M.; Erill, S. *Drug Protein Binding*; Clinical Pharmacology and Therapeutics Series Vol. 6; Praeger: New York, 1984.
(2) Drug–Protein Binding. In: *Ann. N.Y. Acad. Sci.* **1973**, *226* Anton, A. H., Solomon, H. M., Ed.; collected papers of the conference on Drug Protein Binding of the New York Academy of Sciences, Jan 1973.
(3) Meyer, M. C.; Guttman, D. E. *J. Pharm. Sci.* **1968**, *57*, 895–918.
(4) Vallner, J. J. *J. Pharm. Sci.* **1977**, *66*, 447–465.
(5) Sparrow, N. A.; Russell, A. E.; Glasser, L. *Anal. Biochem.* **1982**, *123*, 255–264.
(6) Kurz, H.; Trunk, H.; Weitz, B. *Arzneim.-Forsch/Drug-Res.* **1977**, *27*, 1373–1380.
(7) Sebille, B.; Thuand, N.; Tillement, J. P. *J. Chromatogr.* **1981**, *204*, 285–291.
(8) *Proceedings of the Workshop on Direct Potentiometric Measurements in Blood*; Kock, W. F.; Ed.; National Bureau of Standards: Gaithersburg, MD, May 1983.
(9) Czaban, J. D. *Anal. Chem.* **1985**, *57*, 345A–356A.
(10) Frye, R. M.; Lees, H.; Rechnitz, G. A. *Clin. Biochem.* **1974**, *7*, 258–270.
(11) Andersen, N. F. *Clin. Chem.* **1977**, *23*, 2122–2126.
(12) Naik, D. V.; Jewell, C. F.; Schulman, S. G. *J. Pharm. Sci.* **1975**, *64*, 1243–1245.
(13) Mohanakrishnan, P.; Chignell, C. F. *J. Pharm. Sci.* **1982**, *71*, 1180–1182.
(14) Vadnere, M.; Lindenbaum, S. *Int. J. Pharm.* **1982**, *11*, 57–69.
(15) Kiryu, S.; Oda, Y.; Sasaki, M. *Chem. Pharm. Bull.* **1983**, *31*, 1089–1091.
(16) Birch, B. J.; Clarke, D. E.; Lee, R. S.; Oakes, J. *Anal. Chim. Acta* **1974**, *70*, 417–423.
(17) Kresheck, G. C.; Constantinidis, I. *Anal. Chem.* **1984**, *56*, 152–156.
(18) Hadjiioannou, T. P.; Diamandis, E. P. *Anal. Chim. Acta* **1977**, *94*, 443–447.
(19) Scatchard, G. *Ann. N.Y. Acad. Sci.* **1949**, *51*, 660–673.
(20) Priore, R. L.; Rosenthal, H. E. *Anal. Biochem.* **1976**, *70*, 231–240.
(21) Munson, P. J.; Rodbard, D. *Anal. Biochem.* **1980**, *107*, 220–239.
(22) Klotz, I. M.; Hunston, D. L. *Biochemistry 1971*, *10*, 3065–3069.
(23) Wentworth, W. E. *J. Chem. Educ.* **1965**, *42*, 96–103.
(24) Wentworth, W. E. *J. Chem. Educ.* **1965**, *42*, 162–167.
(25) Marquardt, D. W. *J. Sos. Indust. Appl. Math.* **1963**, *2*, 431–441.
(26) Perrin, C. L. *Mathematics for Chemists*; John Wiley and Sons, Inc.: New York, 1970.
(27) Peters, T., Jr. Serum Albumin. In *The Plasma Proteins*, 2nd ed.; Putnam, F. W., Ed.; Academic Press: New York, 1975, Vol. 1, pp 133–181.
(28) Klotz, I. M. *Science* **1982**, *217*, 1247–1249.

(29) Klotz, I. M. *Biopharm. Drug Dispos.* **1985**, *6*, 105–106.
(30) Deranleau, D. A. *J. Am. Chem. Soc.* **1969**, *91*, 4044–4049.
(31) Deranleau, D. A. *J. Am. Chem. Soc.* **1969**, *91*, 4050–4054.
(32) Benesi, H. A.; Hildebrand, J. H. *J. Am. Chem. Soc.* **1949**, *71*, 2703–2707.
(33) Klotz, I. M. *Arch. Biochem.* **1946**, *9*, 109–117.
(34) Hill, T. L. *J. Chem. Phys.* **1946**, *14*, 441–453.
(35) Bevington, P. R. *Data Reduction and Error Analysis for the Physical Sciences*; McGraw-Hill: New York, 1969.
(36) Teresi, J. D.; Luck, J. M. *J. Biol. Chem.* **1948**, *174*, 653–661.
(37) Diamandis, E. P.; Papastathopoulos, D. S.; Hadjiioannou, T. P. *Clin. Chem.* **1981**, *27*, 427–430.
(38) Christopoulos, T. K.; Diamandis, E. P. *Clin. Biochem.* **1986**, *19*, 151–160.
(39) Koryta, J. *Anal. Chim. Acta* **1988**, *206*, 1–48.

RECEIVED for review August 8, 1989. Accepted October 23, 1989.